

Nanocrystalline and Reusable ZnO Catalyst for the Assembly of Densely Functionalized 4H-Chromenes in Aqueous Medium via One-Pot Three Component Reactions: A Greener “NOSE” Approach

Partha Pratim Ghosh and Asish R. Das*

Department of Chemistry, University of Calcutta, Kolkata-700009, India

S Supporting Information



ABSTRACT: An ecofriendly, one-pot, three component ZnO nanoparticles-mediated synthesis of 4H-chromene in water under thermal condition has been described. The highly product-selective three component electrophilic reaction of 2-hydroxybenzaldehyde with an active methylene compound and another carbon-based varied nature of nucleophile has been developed by a reversible alkylation procedure using greener “NOSE” approach. Greenness of the process was well instituted, as water was used both as reaction media as well as medium for the synthesis of catalyst. In these reactions, the use of nano-ZnO as a catalyst was documented to be crucial for rendering the reactions possible in water media, while replacing nano-ZnO with other acids or bases resulted in the generation of too many side products. The catalyst can be efficiently recycled up to the sixth run, an essential point in the area of green chemistry. The methodology provides cleaner conversion, shorter reaction times, and high selectivity, which make the protocol globally putative. The crystal structures of 4H-chromene, easily produced by a chromatography-free highly product-selective reaction, were explored by means of single crystal X-ray diffraction analysis, and H-bonding arrangements of one signified compound prepared is presented. In optimized mild conditions, the isolated yields are 86–93%.

INTRODUCTION

In recent years, emergent awareness about ecological safety and global warming has caused worldwide concern about the use of renewable sources and reduction of waste. This has shifted the paradigm toward the use of ecofriendly and green protocols in all phases of chemical construction and can be appreciated by creative research that widely addresses the issues of atom economy, economy of steps, and avoidance of hazardous chemicals.¹ Development of efficient and environmentally friendly synthetic methodologies for the synthesis of compound libraries of medicinal scaffolds is as an attractive area of research in both academic and pharmaceutical industry.² Multicomponent reactions (MCR) in water will be one of the most apt approaches, which will meet the requirements of green chemistry as well as for developing libraries of medicinal scaffolds.³

Nanotechnology and related sciences offer the opportunity to make products and processes green from the beginning. The development of green processes and pollutant-free catalysts has integrated great importance. Catalysis lies at the heart of innumerable chemical protocols. Pioneering catalytic processes based on such nanocatalysts will be simpler, economically

efficient, and more ecofriendly, which institutes “green chemistry” and produces most desirable products. The emerging interest on the catalytic properties of transition metal nanoparticles is due to their large surface area, distinctive electronic, magnetic, optical, thermal and chemical properties.⁴ The definite intention to work with nanoparticles is their high catalytic activity, recoverability, improved selectivity, criteria of evolution and role in green chemistry.⁵ Hence, organic synthesis catalyzed by metal/metal oxide nanoparticles has received remarkable importance in recent years.

Chromenes and their structural analogues are of great interest because they are frequently found in a number of natural products and biologically active molecules like antibiotic rhodomyltone, a glycosidase inhibitor myrtucommulone-E and HA14-1, apoptosis inducer (Figure 1).⁶ Their syntheses have attracted wide attention for their biological properties, such as anticonvulsant,⁷ antimicrobial,⁸ antitumor,⁹ anticoagulant, diuretic, spasmolytic, and antianaphylactic activities.¹⁰ On the other hand, 3-substituted coumarin, 3-substituted indole,

Received: April 18, 2013

Published: May 23, 2013

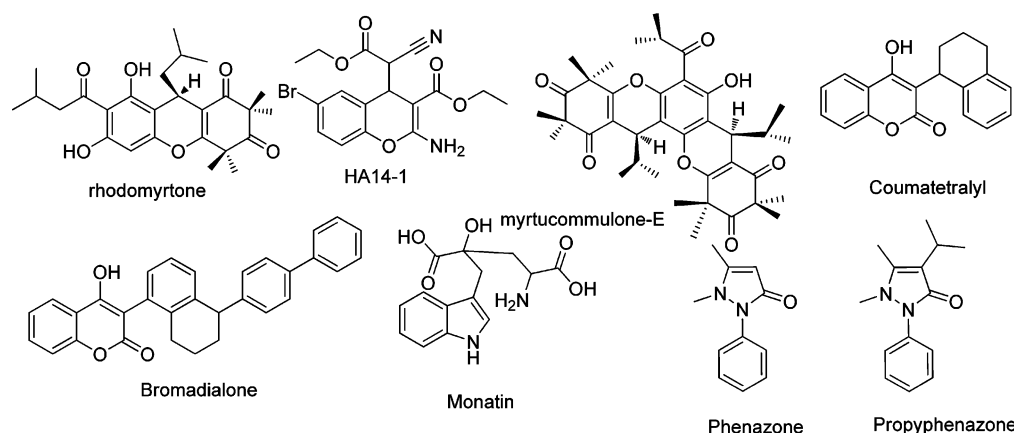
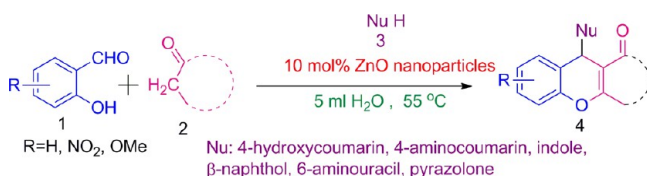


Figure 1. Some biologically active chromenes, coumarins, indole and pyrazolones.

pyrazolone, β -naphthol, uracil derivatives are of much significance due to their presence in plenty of natural and medicinal scaffolds, namely, coumatetralyl,¹¹ bromodialone,¹² monatin,¹³ phenazone,¹⁴ propyphenazone,¹⁵ etc. (Figure 1), possessing antibacterial, anti-HIV, anticancer, antioxidant and antitubercular activities.

A molecular scaffold that accumulates chromene as well as various bioactive nucleophiles like 3-substituted coumarin, 3-substituted indole, pyrazolone, β -naphthol, and 6-aminouracil moieties might integrate properties of both, and the synergism of both the heterocyclic moieties in a single nucleus may result in the formation of some worthwhile molecules from the biological point of view. A literature survey suggested that there are very few reports where chromene assimilates with indole,¹⁶ pyrazolone¹⁷ and 4-hydroxycoumarin¹⁸ moieties. However, the reported methods suffer from many drawbacks like utilization of hazardous chemicals, longer reaction time, unsatisfactory yields and burdensome product isolation procedure. Moreover, the striking disadvantage of almost all reported methods is that the catalysts are consumed in the reaction. To overcome those shortcomings, our interest goes in the growth of nanoparticle-catalyzed organic synthesis enhancement (NOSE) chemistry,¹⁹ which enables us to report ZnO nanoparticles catalyzed synthesis of highly functionalized chromene derivatives via multicomponent reaction approach, commencing with 2-hydroxybenzaldehyde, an active methylene compound and a bioactive carbon-based nucleophile in water (Scheme 1). The

Scheme 1. Synthesis of 4H-Chromene Derivatives



present work materializes as a part of our ongoing research program involving water as the solvent and nano-ZnO as the key catalyst in the synthesis of various biologically active molecules.²⁰

RESULTS AND DISCUSSION

ZnO nanoparticles were prepared through the “bottom up” method.²¹ To characterize ZnO nanoparticles, EDX analysis was performed to determine the elemental composition. EDX

analysis confirmed the presence of zinc and oxygen element only (Figure 2) in the nanosample. The weight % of Zn and O is 73.80 and 26.20, and atomic % is 40.81 and 59.19, respectively.

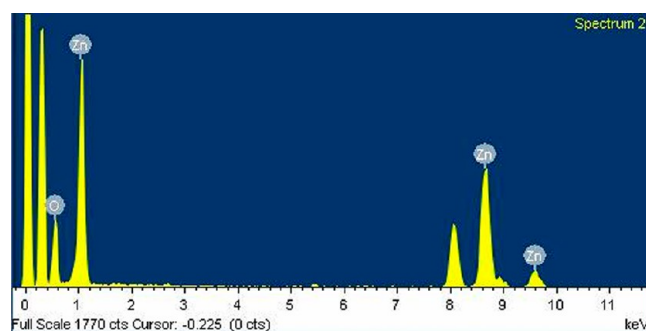


Figure 2. EDX analysis of nano-ZnO.

For the identification of functional groups, bonding information, study of strength and fraction of hydrogen bonding, comparative FT-IR spectra (Figure 3) were recorded between bulk ZnO and nano-ZnO. Broad band at 3408 and 3377 cm^{-1} are assigned to the O–H stretching mode of hydroxyl groups of atmospheric moisture for both nano-ZnO and bulk ZnO, respectively. The peaks at 1631 cm^{-1} of nano-ZnO indicates the presence of C=O residues, probably due to

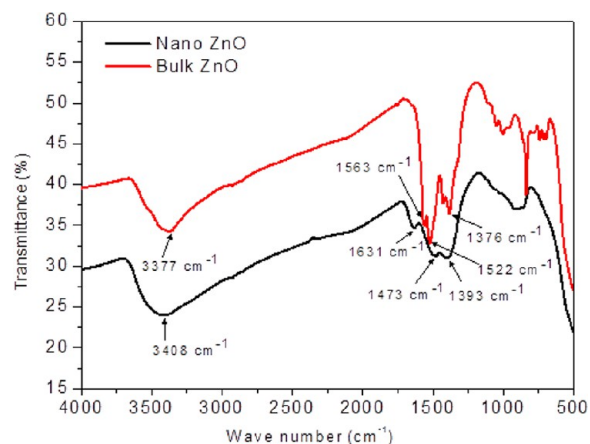


Figure 3. FT-IR spectrum of nano-ZnO.

atmospheric CO₂, which was not observed in bulk ZnO. Hence, as the size of the nanoparticles increases, the content of C=O residues in the sample decreases.

Figure 4 shows the XRD pattern of ZnO nanoparticles. The observed peaks correspond to the Bragg angle for the (100),

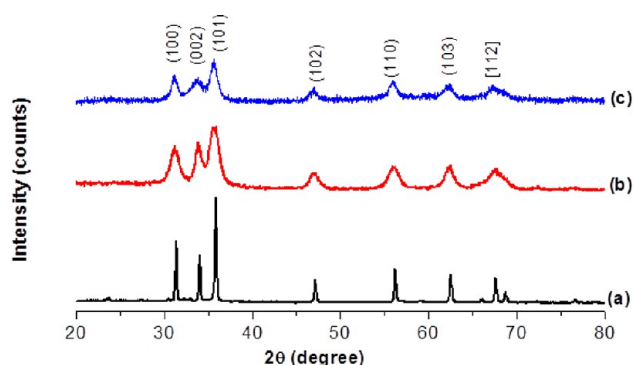


Figure 4. Comparative XRD patterns of (a) bulk ZnO, (b) nano-ZnO, (c) recovered after sixth cycle.

(002), (101), (102), (110), (103) and (112) planes of the crystalline ZnO, which are consistent with standard JCPDS reported values. Applying Sherrer's formula, $D_p = 0.941\lambda/\beta z \cos \theta$; where X-ray wavelength (λ) = 1.5406 Å and β is the corresponding full width at half-maximum (fwhm) value of characteristic peaks (100) and (101), and accordingly, (a) the particle sizes of bulk ZnO is about 68 nm; (b) the synthesized ZnO were found to lie between 10 and 12 nm; and (c) after sixth run of recycling it is about 13–14 nm, conforming the unchanged morphology. These sizes are consistent with those measured from the TEM images, indicating the single crystal nature of nanoparticles.

Figure 5a–c shows the TEM images of synthesized nano-ZnO. The size of the particle of nano-ZnO is estimated through TEM and found to be near about 10 nm. No impurities were involved in the synthesized ZnO nanoparticles sample. The synthesis of ZnO nanoparticles was carried out by aqueous chemical method using zinc acetate dihydrate and potassium hydroxide as source materials. The entire process was carried out in deionized water for its intrinsic advantages, as it is simple, cost-effective, environment-friendly and can be easily scaled up for large scale synthesis; moreover, in this method there is no need to use high pressure and toxic chemicals.

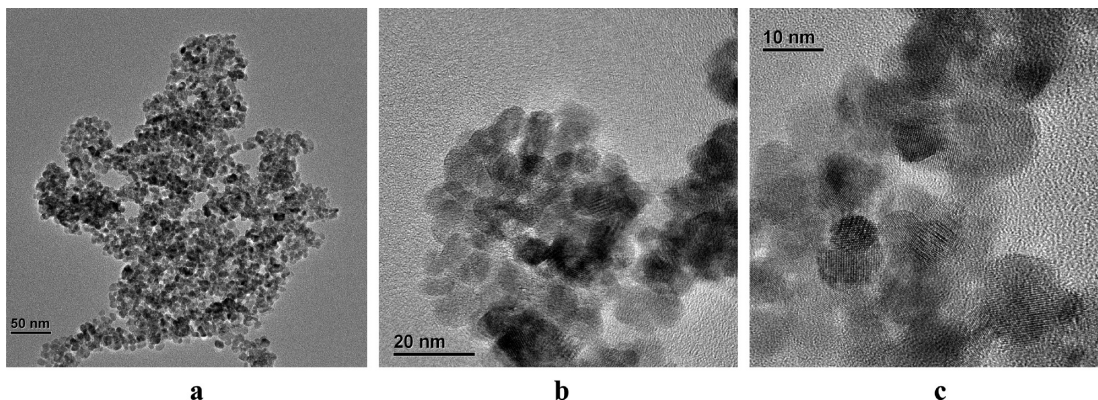


Figure 5. TEM images of nano-ZnO at (a) 50, (b) 20, and (c) 10 nm scale, respectively, in aqueous media.

The TGA and SDTA curve measures the compositional changes associated with the calcinations processes and is shown in Figure 6. Because of high thermal stability of nano-ZnO, no change has been observed up to 600 °C.

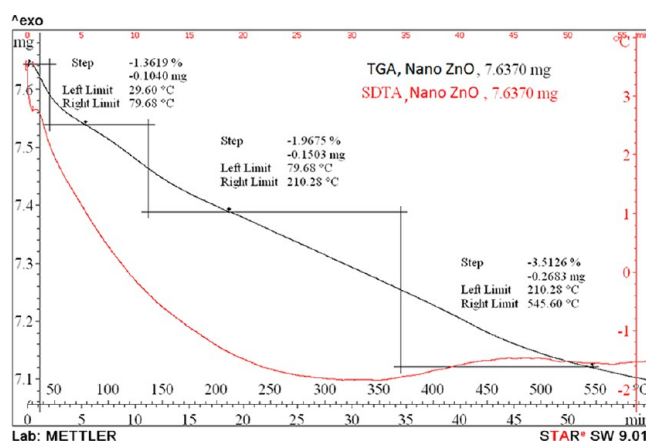


Figure 6. TGA and SDTA curve of nano-ZnO.

In order to confirm ZnO nanoparticles to be the crucial for rendering the reactions possible in aqueous media, we carried out a long screening test employing a series of catalysts and solvents (Table 1). Initially, salicylaldehyde (1.0 mmol), dimedone (1.0 mmol), and 4-hydroxycoumarin (1.0 mmol) were refluxed in presence of H₂O and ethanol as the solvent without any catalyst; however, the reactions, even after 24 h, failed to generate any product (Table 1, entries 1 and 2). Then the reaction was carried out in water in the presence of *p*-toluenesulphonic acid (PTSA) at 55 °C, and the product was isolated in 41% yield (Table 1, entry 3). The reactions were also restrained in aqueous media by using L-proline as the catalyst (Table 1, entries 4), while the use of zeolite as a catalyst in aqueous media provided a trace amount of the desired product (Table 1, entry 5). Among the Lewis acid catalysts, InCl₃ was tested, but it did not promote the reaction well (Table 1, entries 6). However, an improved yield was obtained when we applied metal oxide like nano-MgO, nano-Al₂O₃ and bulk ZnO as catalyst in water (Table 1, entries 7, 8 and 9). Interestingly, we observed that ZnO was most effective for the selective formation of desired product. Again ZnO nanoparticles showed outstanding activity in the formation of desired product than bulk ZnO in terms of reaction time and

Table 1. Screening of Catalyst, Solvents, and Reaction Conditions^a

entry	catalysts	solvents	conditions (°C)	time (h)	yields ^b (%)
1	–	H ₂ O	reflux	24	– ^c
2	–	EtOH	reflux	24	– ^c
3	TsOH (10 mol %)	H ₂ O	55	8	41
4	L-proline (10 mol %)	H ₂ O	55	8	46
5	zeolite (10 mol %)	H ₂ O	55	8	trace
6	InCl ₃ (10 mol %)	H ₂ O	55	8	29
7	nano-MgO (10 mol %)	H ₂ O	55	8	51
8	nano-Al ₂ O ₃ (10 mol %)	H ₂ O	55	8	55
9	bulk ZnO (10 mol %)	H ₂ O	55	8	68
10	nano-ZnO (10 mol %)	H₂O	55	45 min	92
11	nano-ZnO (5 mol %)	H ₂ O	55	45 min	81
12	nano-ZnO (15 mol %)	H ₂ O	55	45 min	87
13	nano-ZnO (10 mol %)	EtOH	55	45 min	77
14	nano-ZnO (10 mol %)	CH ₃ CN	55	45 min	56
15	nano-ZnO (10 mol %)	CHCl ₃	55	45 min	31

^aAll reactions were carried out with salicylaldehyde (1.0 mmol), dimedone (1.0 mmol), and 4-hydroxycoumarin (1.0 mmol) in 5 mL of solvent. ^bYield of isolated product. ^cReaction failed to provide any product.

temperature, and eventually we achieved satisfaction because the reaction proceeded well, affording the desired product in 92% yield within 45 min (Table 1, entry 10). The reaction was very clean because of the amphoteric nature of nano-ZnO; besides, upon application of acids or bases, many unwanted products in the reaction flask have been generated because of the high acid–base sensitivity of starting materials, specifically carbon-based nucleophiles.

Ascertaining nano-ZnO as the right catalyst for the experiment, we then concentrated our attention on designing and also generalizing the favorable conditions for the reaction. We first attempted some screening tests with nano-ZnO. The quantity of the catalyst had a large effect on the formation of the desired product. The use of 5 mol % nano-ZnO diminished the quantity of the yield, whereas the yield of the product also decreased when we used 15 mol % nano-ZnO (Table 1, entries 11 and 12). Water (Table 1, entry 10) has shown its superiority to other solvents tested [ethanol (Table 1, entry 13), acetonitrile (Table 1, entry 14) and chloroform (Table 1, entry 15)]. As a part of our program aimed in developing new and environmentally benign synthetic methodologies with ZnO nanoparticles, these optimized conditions were then applied for all experiments: taking equimolar amounts of 2-hydroxy benzaldehyde (**1**), active methylene compound (**2**) and a carbon-based nucleophile (**3**) at 55 °C in the presence of 10 mol % nano-ZnO in aqueous media (Scheme 1). Typically, a mixture of 2-hydroxy benzaldehyde (1.0 mmol), active methylene compound (1.0 mmol) and a carbon-based nucleophile (1.0 mmol) and 10 mol % nano-ZnO in 3 mL of water was refluxed for 40–65 min, which afforded a library of

4H-chromene derivatives (**4**) in good to excellent yields (85–93%) (Table 2).

To estimate the scope and generality of the protocol, 2-hydroxy aromatic aldehydes, having both electron-withdrawing and electron-donating groups, were reacted with an active methylene compound like dimedone, 1,3-cyclohexanedione, malononitrile and *N,N*-dimethylbarbituric acid and a carbon-based nucleophile like 4-hydroxycoumarin, 4-aminocoumarin, 6-aminouracil, β -naphthol, indole and pyrazolone under optimized reaction conditions, and the results are exhibited in Table 2. The reactions were consistently carried out at the 1 mmol scale, and no change of product yield was observed when scaled up to the 10 mmol scale. From the perspective of green chemistry, it was positive to find that the final products could be isolated by filtration because of their solubility difference of the product from the starting materials, leading to separation of product from the reaction mixture upon completion, thereby facilitating easy isolation of solid product from the reaction mixture simply by filtration. Since ZnO nanoparticles are often recovered easily by simple workup, which prevents contamination of products, they may be considered as promising safe and reusable catalysts as well as being greener compared to traditional catalysts. Furthermore, the purity of the products was too high to require their preparation in an analytically pure form by single recrystallization, thus avoiding extraction steps and chromatographic separations. Therefore, we preferred water as the reaction medium over unsafe organic solvents, which decreases the chemical impurity, features easy workup procedure, and minimizes large volumes of waste from the discarded chromatographic static phases. The structure of the final products were well characterized by using spectral (IR, ¹H, ¹³C NMR and HRMS) and elemental analysis data. The structural motif was fully established by single X-ray crystallographic analysis of one signified compound **4e** (CCDC 926789) (Figure 7).²² The compound **4e** crystallizes in the triclinic P $\bar{1}$ space group with one molecule in the asymmetric unit (*Z* = 2). While the molecule in the asymmetric unit as such had no conventional functional groups to form H-bonding, the coumarin groups present, however, were responsible for the formation of weak intermolecular H-bonding along *c*-direction. The inversion related molecule in the asymmetric unit forming the heterochiral dimer synthon through C–H \cdots O interaction is shown in Figure 8. They formed channels with one molecule above and one molecule below via C–H \cdots O interaction and are stabilized by aromatic C–H \cdots π interactions.

Presumably the reaction seems to proceed through following mechanistic pathway as presented in Scheme 2. The ZnO nanoparticles facilitate the Knoevenagel-type coupling through Lewis acid sites (Zn²⁺) coordinated to the oxygen of carbonyl groups of 2-hydroxybenzaldehyde. On the other hand, ZnO nanoparticles can activate active methylene compounds so that deprotonation of the C–H bond occurs in the presence of Lewis basic sites (O²⁻) and form intermediate (I). Subsequently, during the Michael addition step, nucleophilic attack on intermediate (I) by the carbon-based nucleophile afforded the desired product (**4**) via intermediate (II) paving the way for its ring closure. Alternatively, there is another possible reaction pathway for the reaction, via the formation of intermediate (III) followed by its reaction with dimedone to afford **4**. Our efforts to isolate intermediate (III) from the two-component reaction of 2-hydroxybenzaldehyde (1 equiv) and 4-hydroxycoumarin (1 equiv) in water in presence of nano-ZnO did not fructify. These reactions, instead, led to (i)

Table 2. Substrate Scopes for the Synthesis of 4*H*-Chromenes^a

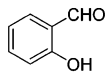
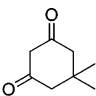
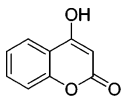
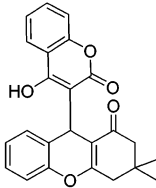
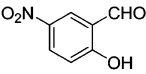
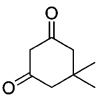
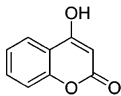
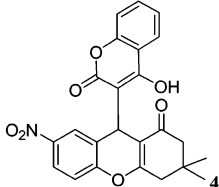
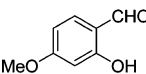
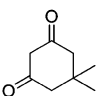
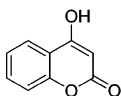
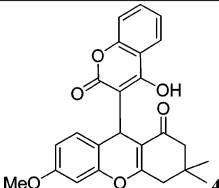
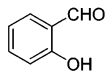
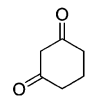
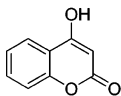
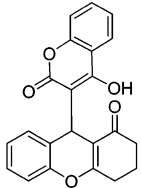
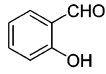
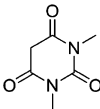
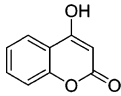
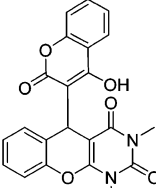
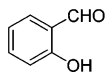
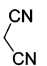
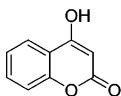
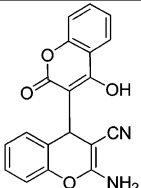
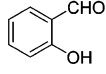
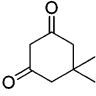
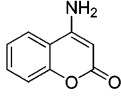
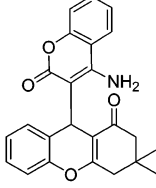
Entry	Aldehyde	Active methylene compound	Nucleophile	Products	t(min)	Yields ^b
1				 4a	45	92
2				 4b	40	90
3				 4c	45	91
4				 4d	45	91
5				 4e	40	91
6				 4f	40	87
7				 4g	45	90

Table 2. continued

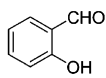
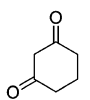
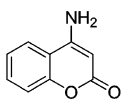
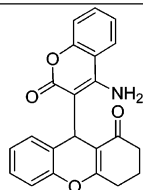
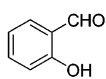
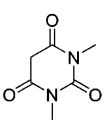
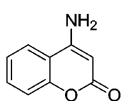
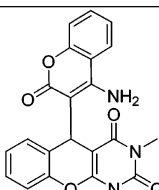
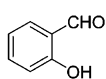
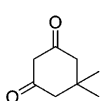
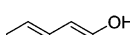
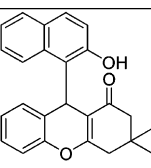
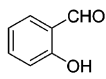
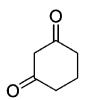
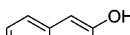
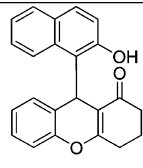
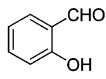
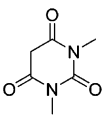
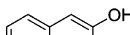
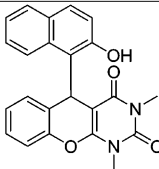
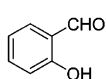
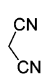
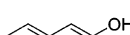
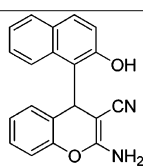
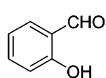
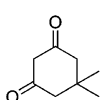
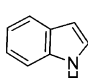
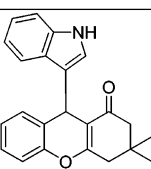
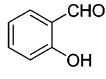
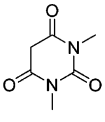
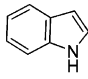
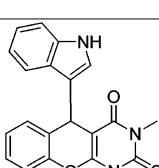
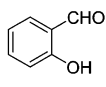
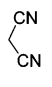
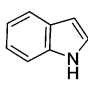
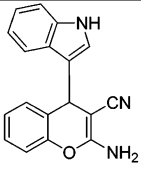
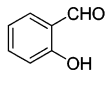
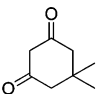
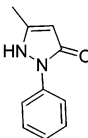
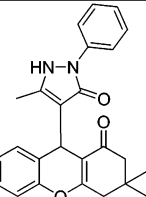
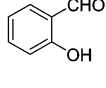
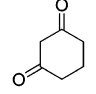
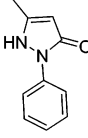
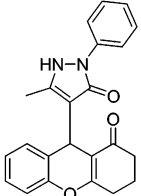
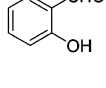
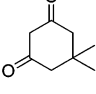
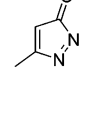
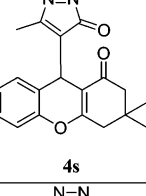
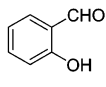
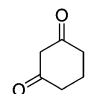
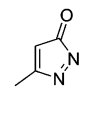
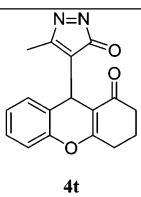
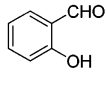
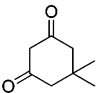
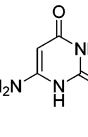
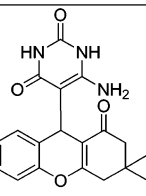
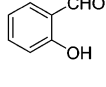
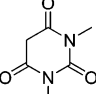
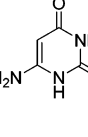
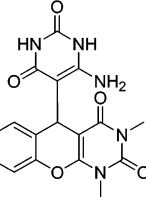
Entry	Aldehyde	Active methylene compound	Nucleophile	Products	t(min)	Yields ^b
8				 4h	45	90
9				 4i	50	91
10				 4j	55	93
11				 4k	45	91
12				 4l	50	92
13				 4m	45	93
14				 4n	50	91
15				 4o	50	91

Table 2. continued

Entry	Aldehyde	Active methylene compound	Nucleophile	Products	t(min)	Yields ^b
16				 4p	40	90
17				 4q	50	88
18				 4r	50	90
19				 4s	50	90
20				 4t	40	89
21				 4u	60	86
22				 4v	65	85

^a2-Hydroxy benzaldehyde (1 mmol), active methylene compound (1 mmol), and a nucleophile (1 mmol) were stirred in 5 mL of water in the presence of 10 mol % nano-ZnO. ^bIsolated yield of the pure product.

(Figure 6) (Ar = 2-OHC₆H₄) with 50% unreacted 2-hydroxybenzaldehyde. Similarly, the reaction of equimolar

amounts of dimedone (1 equiv) and 2-hydroxybenzaldehyde (1 equiv) was performed with a view to getting intermediate

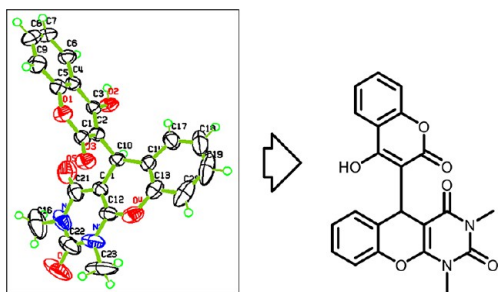


Figure 7. ORTEP diagram of one signified compound **4e** (CCDC 926789).

(I). Interestingly, this reaction resulted in the formation of (ii) (Figure 6) along with unreacted 2-hydroxybenzaldehyde, wherein intermediate (I) could not be detected even in traces. These results indicate that both intermediates (III) and (I) in the above reactions are very reactive toward the subsequent reactions with dimedone and 4-hydroxycoumarin, respectively. Hence information on the relative rates of formation as well as further reactions of intermediate (III) and (I) with dimedone and 4-hydroxycoumarin, respectively, could not be obtained and compared. Consequently, whether the multicomponent reactions occur through intermediate (I) or (III), it could not be ascertained in the current study.

It is pertinent to mention that the reaction is highly product-selective, affording only desired product (**4**); surprisingly, (i)–(v) (Figure 9) were not observed in detectable amounts at all applying this reaction.

It is important to emphasize that catalyst recyclability is an essential aspect of green chemistry. The catalyst could be recycled easily followed by washing with ethanol several times to remove all the organic substances. It was then dried at room temperature and was recycled six consecutive times with almost unaltered catalytic activity. The recyclability chart of the catalytic potential of the nano-ZnO is shown in Figure 10 (recovery amount 92% and yield, 89% after sixth run) (Table 2, entry 1). The XRD pattern of the fresh nano-ZnO was compared with the recovered one after the sixth cycle, and bulk ZnO (Figure 4) and the TEM image of recovered nano-ZnO after sixth cycle is presented in Figure 11.

CONCLUSION

In conclusion, a highly product-selective and chromatography-free three component reaction protocol has been developed for the synthesis of densely functionalized 4*H*-chromene derivatives, catalyzed by ZnO nanoparticles effectively in aqueous

medium using “NOSE” approach. ZnO nanoparticles were well characterized by EDX, TEM, FT-IR and XRD techniques, and their thermal stability was confirmed by TGA and SDTA curve. This method offers several advantages including shorter reaction time with excellent yields, a simple workup procedure, ease of separation and recyclability of the catalyst, as well as the ability to tolerate a wide variety of 2-hydroxy benzaldehyde, active methylene compounds and carbon-based biologically important nucleophile. Several green chemistry principles were included, as (i) it is a one-pot multicomponent reaction offering only water as the byproduct (ii) using commercially available substrates with low cost and (iii) easy extension of the substrate scope. Finally, one representative molecular structure was investigated by means of X-ray diffraction analysis, which confirms the presence of weak intermolecular H-bonding forming a molecular channel.

EXPERIMENTAL SECTION

Preparation of ZnO Nanoparticles. To a 50 mL 0.05 M solution of zinc acetate dihydrate in deionized water, 25 mL 1 M aqueous solution of KOH was added dropwise with a dropping funnel for 1 h at 60 °C under sonication. The sonication was carried out for another 1 h. Then the solution was centrifuged, the mother liquor was removed, and the precipitate was washed five times with deionized water. Then the precipitate was dried in air. It was characterized by TEM image and X-ray diffraction study.

General Procedure for the Synthesis of 4*H*-Chromene Derivatives (4a**–**4v**).** A mixture of 2-hydroxybenzaldehyde **1** (1 mmol), an active methylene compound **2** (1 mmol), carbon-based nucleophile **3** (1 mmol) and 10 mol % ZnO nanoparticles in 5 mL of water was stirred at 55 °C for the stipulated time mentioned in Table 2. After completion of the reaction (indicated by TLC), the free-flowing solid was filtered and washed with water (20 mL) to afford the desired products as pale yellow solids. The product thus obtained was recrystallized from ethanol to get pure compounds as white or pale yellow crystals. The isolated compounds were well characterized by IR, ¹H NMR, ¹³C NMR, HRMS, elemental analysis and an X-ray crystallographic study.

9-(4-Hydroxy-2-oxo-2*H*-chromen-3-yl)-3,3-dimethyl-2,3,4,9-tetrahydro-1*H*-xanthen-1-one (4a**).** Yield: (0.357g, 92%); White crystalline solid; mp 232–234 °C; IR (KBr) 3317, 3192, 2952, 2921, 1674, 1632, 1582, 1486, 1453, 1369, 1275, 1234, 1184, 1036, 1014, 758 cm⁻¹; δ_H (300 MHz; DMSO-*d*₆; Me₄Si) δ 0.96 (s, 3H), 1.03 (s, 3H), 2.06–2.23 (m, 2H), 2.46–2.52 (m, 2H), 5.32 (s, 1H), 6.87–7.09 (m, 5H), 7.17 (t, *J* = 7.5 Hz, 1H), 7.40 (t, *J* = 7.5 Hz, 1H), 7.92 (d, *J* = 6 Hz, 1H); δ_C (75 MHz, DMSO-*d*₆; Me₄Si) δ 25.6, 26.4, 27.8, 30.6, 49.1, 114.4, 114.5, 115.4, 122.1, 122.6, 123.1, 126.22, 127.3, 129.9, 151.2, 158.9, 166.8, 196.1; HRMS (ESI-TOF) Calcd for C₂₄H₂₀O₅ ([*M* + *H*]⁺) 389.1344, found 389.1341. Anal. Calcd for C₂₄H₂₀O₅: C 74.21; H 5.19%. Found: C 74.17; H 5.17%.

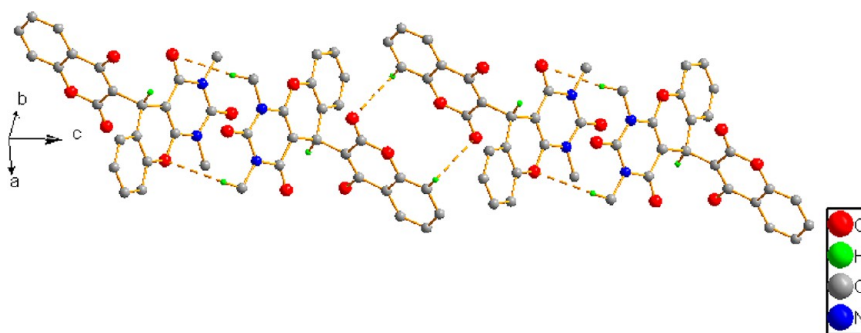


Figure 8. The intermolecular H-bonds between the *R*-molecules and *S*-molecules. All hydrogens, except those participating in the H-bonding, have been omitted for clarity. Symmetry codes: A *x*, *y*, $-1 + x$; B $2 - x$, $-y$, $-z$; C $2 - x$, $-y$, $1 - z$.

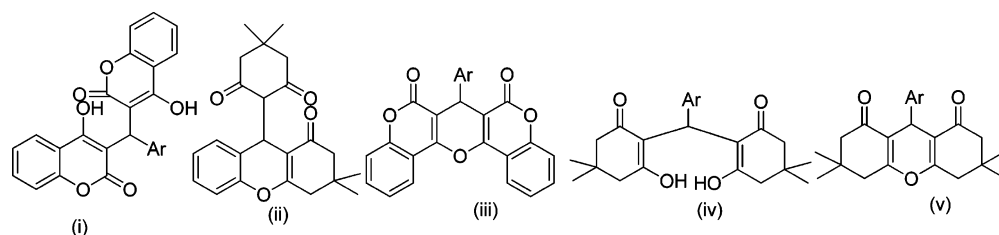
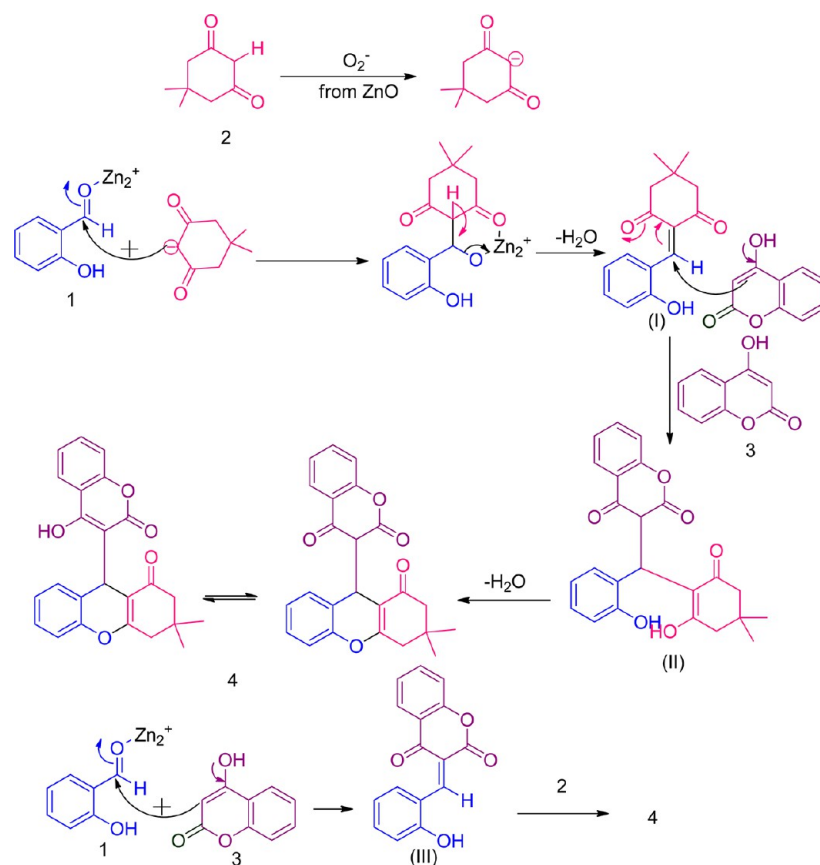
Scheme 2. Plausible Mechanism for the Formation of 4*H*-Chromene

Figure 9. Condensation products of aromatic aldehyde with 4-hydroxycoumarin/dimedone.

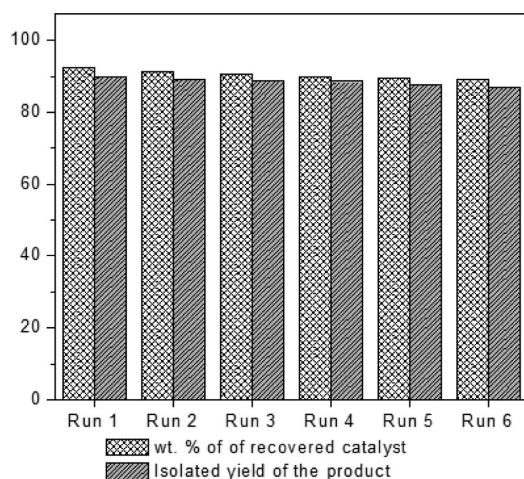


Figure 10. Recyclability chart of ZnO nanoparticles.

9-(4-Hydroxy-2-oxo-2*H*-chromen-3-yl)-3,3-dimethyl-7-nitro-2,3,4,9-tetrahydro-1*H*-xanthen-1-one (4b). Yield: (0.390g, 90%);

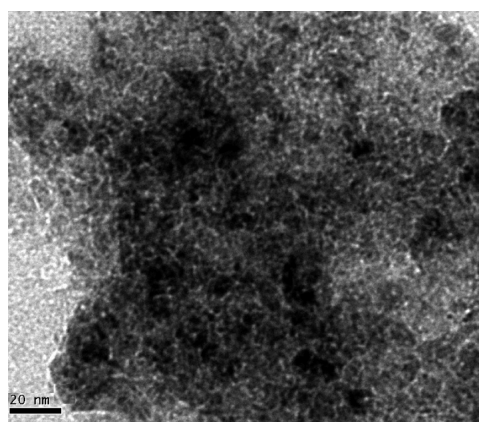


Figure 11. TEM image of recovered nano-ZnO after sixth cycle.

Pale yellow crystalline solid; mp 222–224 °C; IR (KBr) 3321, 3191, 2950, 1679, 1636, 1581, 1484, 1366, 1273, 1184, 1034, 1015, 758 cm^{-1} ; δ_H (300 MHz; DMSO- d_6 ; Me $_4$ Si) δ 0.90 (s, 3H), 1.02 (s, 3H), 2.10–2.19 (m, 2H), 2.32–2.49 (m, 2H), 5.09 (s, 1H), 7.08–7.13 (m,

2H), 7.35 (t, $J = 7.5$ Hz, 1H), 7.66 (s, 1H), 7.75–8.00 (m, 3H); δ_C (75 MHz, DMSO- d_6 ; Me $_4$ Si) δ 26.9, 29.3, 31.8, 32.1, 50.6, 103.1, 111.1, 112.8, 115.1, 115.6, 116.4, 120.4, 123.3, 124.6, 125.6, 127.2, 130.8, 139.8, 152.8, 168.8, 196.8; HRMS (ESI-TOF) Calcd for C $_{24}$ H $_{19}$ NO $_7$ ([M + H] $^+$) 434.1195, found 434.1190. Anal. Calcd for C $_{24}$ H $_{19}$ NO $_7$: C 66.51; H 4.42; N 3.23%. Found: C 66.49; H 4.44; N 3.21%.

9-(4-Hydroxy-2-oxo-2H-chromen-3-yl)-6-methoxy-3,3-dimethyl-2,3,4,9-tetrahydro-1H-xanthen-1-one (4c). Yield: (0.380g, 91%); White crystalline solid; mp 246–248 °C; IR (KBr) 3320, 3196, 2951, 1678, 1633, 1581, 1482, 1452, 1362, 1271, 1182, 1033, 1015, 757 cm $^{-1}$; δ_H (300 MHz; DMSO- d_6 ; Me $_4$ Si) δ 0.97 (s, 3H), 1.10 (s, 3H), 1.98–2.19 (m, 2H), 2.26–2.47 (m, 2H), 3.61 (s, 3H), 5.30 (s, 1H), 6.38–7.47 (m, 6H), 7.90 (s, 1H); δ_C (75 MHz, DMSO- d_6 ; Me $_4$ Si) δ 18.8, 25.2, 27.0, 28.2, 29.5, 31.9, 32.1, 50.7, 55.5, 56.7, 100.8, 110.7, 111.6, 117.9, 122.8, 123.4, 124.3, 129.5, 131.3, 131.9, 151.0, 158.4, 158.9, 165.0, 196.4; HRMS (ESI-TOF) Calcd for C $_{25}$ H $_{22}$ O $_6$ ([M + H] $^+$) 419.1450, found 419.1448. Anal. Calcd for C $_{25}$ H $_{22}$ O $_6$: C, 71.76; H, 5.30; %. Found: C, 71.73; H, 5.28%.

9-(4-Hydroxy-2-oxo-2H-chromen-3-yl)-2,3,4,9-tetrahydro-1H-xanthen-1-one (4d). Yield: (0.327g, 91%); White crystalline solid; mp 207–209 °C; IR (KBr) 3320, 3199, 2955, 1671, 1633, 1581, 1481, 1451, 1361, 1277, 1181, 1036, 1017, 758 cm $^{-1}$; δ_H (300 MHz; DMSO- d_6 ; Me $_4$ Si) δ 1.60–1.90 (m, 2H), 2.33 (s, 2H), 2.63 (s, 2H), 5.54 (s, 1H), 6.66 (d, $J = 6.6$ Hz, 1H), 7.03–7.19 (m, 2H), 7.36–7.41 (m, 2H), 7.58 (d, $J = 9$ Hz, 2H), 7.74 (d, $J = 9$ Hz, 1H); δ_C (75 MHz, DMSO- d_6 ; Me $_4$ Si) δ 28.2, 29.3, 29.5, 31.6, 32.0, 50.7, 100.1, 110.1, 110.3, 111.2, 115.6, 122.5, 124.2, 126.1, 127.2, 128.1, 128.6, 129.2, 133.2, 150.3, 165.0, 196.4; HRMS (ESI-TOF) Calcd for C $_{22}$ H $_{16}$ O $_5$ ([M + H] $^+$) 361.1076, found 361.1071. Anal. Calcd for C $_{22}$ H $_{16}$ O $_5$: C 73.33; H 4.48%. Found: C 73.30; H 4.41%.

5-(4-Hydroxy-2-oxo-2H-chromen-3-yl)-1,3-dimethyl-1H-chromeno[2,3-d]pyrimidine-2,4(3H,5H)-dione (4e). Yield: (0.367g, 91%); White crystalline solid; mp 267–269 °C; IR (KBr) 3407, 3160, 3079, 1730, 1640, 1577, 1431, 1394, 1340, 1237, 1187, 1136, 1039, 757 cm $^{-1}$; δ_H (300 MHz; DMSO- d_6 ; Me $_4$ Si) δ 3.43 (s, 3H), 3.61 (s, 3H), 5.37 (s, 1H), 7.10–7.61 (m, 6H), 8.00–8.04 (m, 2H); δ_C (75 MHz, DMSO- d_6 ; Me $_4$ Si) δ 28.1, 28.6, 29.1, 29.5, 29.6, 36.2, 87.1, 108.9, 115.9, 116.2, 116.9, 121.9, 123.8, 124.3, 125.5, 125.8, 126.1, 128.5, 131.7, 149.9, 150.9, 161.9, 165.4, 196.4; HRMS (ESI-TOF) Calcd for C $_{22}$ H $_{16}$ N $_2$ O $_6$ ([M + H] $^+$) 405.1042, found 405.1046. Anal. Calcd for C $_{22}$ H $_{16}$ N $_2$ O $_6$: C 65.34; H 3.99, N 6.93%. Found: C 65.37; H 3.94, N 6.90%.

2'-Amino-4-hydroxy-2-oxo-2H,4'H-[3,4'-bichromene]-3'-carbonitrile (4f). Yield: (0.332g, 87%); White crystalline solid; mp 200–202 °C; IR (KBr) 3440, 3366, 2181, 1668, 1618, 1576, 1531, 1481, 1184, 1034, 751 cm $^{-1}$; δ_H (300 MHz; DMSO- d_6 ; Me $_4$ Si) δ 5.30 (s, 1H), 5.79 (s, 2H), 6.80–7.19 (m, 4H), 7.27–7.59 (m, 2H), 7.62–7.94 (m, 2H); δ_C (75 MHz, DMSO- d_6 ; Me $_4$ Si) δ 30.5, 115.6, 116.0, 116.3, 116.5, 121.1, 121.9, 123.6, 123.8, 124.2, 127.8, 128.1, 131.7, 132.2, 149.8, 152.8, 162.3; HRMS (ESI-TOF) Calcd for C $_{19}$ H $_{12}$ N $_2$ O $_4$ ([M + H] $^+$) 333.0831, found 333.0827. Anal. Calcd for C $_{19}$ H $_{12}$ N $_2$ O $_4$: C, 68.67; H, 3.64; N, 8.43; O, 19.26%. Found: C, 68.63; H, 3.61; N, 8.48; O, 19.21%.

9-(4-Amino-2-oxo-2H-chromen-3-yl)-3,3-dimethyl-2,3,4,9-tetrahydro-1H-xanthen-1-one (4g). Yield: (0.349g, 90%); White crystalline solid; mp 254–256 °C; IR (KBr) 3401, 3162, 3078, 1732, 1641, 1571, 1435, 1398, 1341, 1231, 1139, 1032, 758 cm $^{-1}$; δ_H (300 MHz; DMSO- d_6 ; Me $_4$ Si) δ 0.98 (s, 3H), 1.05 (s, 3H), 2.05–2.26 (m, 2H), 2.41–2.57 (m, 2H), 5.13 (s, 1H), 6.94–7.14 (m, 4H), 7.25 (t, $J = 7.5$ Hz, 1H), 7.47 (t, $J = 7.5$ Hz, 2H), 8.08 (d, $J = 6$ Hz, 1H); δ_C (75 MHz, DMSO- d_6 ; Me $_4$ Si) δ 27.1, 28.5, 29.4, 32.1, 50.8, 101.2, 110.2, 115.6, 116.5, 123.8, 124.3, 124.6, 127.5, 128.9, 150.7, 152.7, 166.3, 196.9; HRMS (ESI-TOF) Calcd for C $_{24}$ H $_{21}$ NO $_4$ ([M + H] $^+$) 388.1504, found 388.1501. Anal. Calcd for C $_{24}$ H $_{21}$ NO $_4$: C 74.40; H 5.46; N 3.62%. Found: C 74.37; H 5.49 N 3.58%.

9-(4-Amino-2-oxo-2H-chromen-3-yl)-2,3,4,9-tetrahydro-1H-xanthen-1-one (4h). Yield: (0.357g, 91%); White crystalline solid; mp 232–234 °C; IR (KBr) 3389, 3170, 3098, 1741, 1641, 1579, 1436, 1390, 1346, 1238, 1137, 1039, 758 cm $^{-1}$; δ_H (300 MHz; DMSO- d_6 ; Me $_4$ Si) δ 1.99–2.06 (m, 2H), 2.18–2.19 (m, 2H), 2.31–2.42 (m, 2H),

4.91 (s, 1H), 6.73–6.99 (m, 4H), 7.13–7.16 (m, 2H), 7.23–7.48 (m, 4H); δ_C (75 MHz, DMSO- d_6 ; Me $_4$ Si) δ 26.4, 27.2, 33.3, 34.1, 36.6, 103.3, 106.2, 115.5, 120.7, 122.4, 125.9, 126.5, 127.9, 131.6, 134.9, 136.5, 146.0, 147.7, 149.3, 152.4, 162.0, 164.2, 164.5, 168.2; HRMS (ESI-TOF) Calcd for C $_{22}$ H $_{17}$ NO $_4$ ([M + H] $^+$) 360.1191, found 360.1187. Anal. Calcd for C $_{22}$ H $_{17}$ NO $_4$: C 73.53; H 4.77; N 3.90%. Found: C 73.56; H 4.72; N 3.88%.

9-(4-Amino-2-oxo-2H-chromen-3-yl)-2,3,4,9-tetrahydro-1H-xanthen-1-one (4i). Yield: (0.366g, 91%); White crystalline solid; mp 225–227 °C; IR (KBr) 3444, 3178, 1740, 1631, 1570, 1438, 1397, 1348, 1239, 1188, 1135, 1031, 758 cm $^{-1}$; δ_H (300 MHz; DMSO- d_6 ; Me $_4$ Si) δ 3.13–3.16 (m, 3H), 3.21 (s, 3H), 5.30 (s, 1H), 6.91–7.88 (m, 6H), 8.10–8.18 (m, 2H); δ_C (75 MHz, DMSO- d_6 ; Me $_4$ Si) δ 24.3, 25.1, 80.77, 108.25, 109.69, 110.74, 111.5, 111.9, 113.2, 114.2, 117.6, 121.6, 123.7, 126.9, 128.7, 130.9, 145.4, 149.0, 149.5, 150.7, 198.7; HRMS (ESI-TOF) Calcd for C $_{22}$ H $_{17}$ N $_3$ O $_5$ ([M + H] $^+$) 404.1202, found 404.1207. Anal. Calcd for C $_{22}$ H $_{17}$ N $_3$ O $_5$: C 65.5; H 4.25; N 10.42%. Found: C 65.44; H 4.21 N 10.46%.

9-(2-Hydroxynaphthalen-1-yl)-3,3-dimethyl-2,3,4,9-tetrahydro-1H-xanthen-1-one (4j). Yield: (0.344g, 93%); White crystalline solid; mp 234–236 °C; IR (KBr) 3398, 3210, 2870, 1636, 1598, 1481, 1390, 1199, 1151, 1036, 758 cm $^{-1}$; δ_H (300 MHz; DMSO- d_6 ; Me $_4$ Si) δ 0.85 (s, 3H), 0.99 (s, 3H), 2.03–2.24 (m, 2H), 2.41–2.57 (m, 2H), 5.64 (s, 1H), 6.44–6.48 (m, 2H), 6.63–6.66 (m, 4H), 6.77 (t, $J = 7.5$ Hz, 1H), 7.18–7.32 (d, $J = 6$ Hz, 1H), 7.62–7.67 (m, 2H), 8.02 (d, $J = 6$ Hz, 1H), 9.26 (s, 1H); δ_C (75 MHz, DMSO- d_6 ; Me $_4$ Si) δ 26.9, 28.5, 29.4, 32.3, 50.6, 113.6, 116.9, 117.3, 118.3, 120.1, 123.8, 125.0, 127.1, 128.7, 129.8, 131.3, 132.2, 147.5, 153.6, 165.2, 197.6; HRMS (ESI-TOF) Calcd for C $_{25}$ H $_{22}$ O $_3$ ([M + H] $^+$) 371.1602, found 371.1599. Anal. Calcd for C $_{25}$ H $_{22}$ O $_3$: C 81.06; H 5.99%. Found: C 81.03; H 5.94%.

9-(2-Hydroxynaphthalen-1-yl)-2,3,4,9-tetrahydro-1H-xanthen-1-one (4k). Yield: (0.311g, 91%); White crystalline solid; mp 211–213 °C; IR (KBr) 3392, 3238, 2970, 1627, 1598, 1487, 1398, 1196, 1154, 1048, 757 cm $^{-1}$; δ_H (300 MHz; DMSO- d_6 ; Me $_4$ Si) δ 1.55–1.58 (m, 2H), 1.86–1.87 (m, 2H), 2.16 (d, $J = 3$ Hz, 2H), 5.64 (s, 1H), 7.11–7.25 (m, 2H), 7.33–7.49 (m, 2H), 7.56–7.60 (m, 2H), 7.73–7.75 (d, $J = 6$ Hz, 2H), 7.87 (d, $J = 7.5$ Hz, 2H); δ_C (75 MHz, DMSO- d_6 ; Me $_4$ Si) δ 29.4, 31.3, 32.4, 32.8, 50.6, 105.4, 106.4, 115.5, 118.0, 120.5, 121.0, 123.3, 123.7, 128.4, 130.9, 131.3, 135.0, 138.0, 146.6, 151.9, 162.2, 163.6, 164.3, 196.0; HRMS (ESI-TOF) Calcd for C $_{23}$ H $_{18}$ O $_3$ ([M + H] $^+$) 343.1289, found 343.1286. Anal. Calcd for C $_{23}$ H $_{18}$ O $_3$: C 80.68; H 5.30%. Found: C 80.62; H 5.27%.

5-(2-Hydroxynaphthalen-1-yl)-1,3-dimethyl-1H-chromeno[2,3-d]pyrimidine-2,4(3H,5H)-dione (4l). Yield: (0.357g, 92%); White crystalline solid; mp 192–194 °C; IR (KBr) 3418, 3222, 2978, 1628, 1592, 1488, 1392, 1192, 1157, 1041, 759 cm $^{-1}$; δ_H (300 MHz; DMSO- d_6 ; Me $_4$ Si) δ 3.34 (s, 3H), 3.60 (s, 3H), 5.97 (s, 1H), 6.78–7.14 (m, 5H), 7.19–7.36 (m, 2H), 7.50–7.69 (m, 3H), 9.83 (s, 1H); δ_C (75 MHz, DMSO- d_6 ; Me $_4$ Si) δ 28.6, 30.7, 89.4, 109.4, 115.8, 117.9, 121.0, 122.3, 122.7, 122.8, 123.5, 124.6, 125.8, 126.4, 127.7, 128.4, 128.8, 129.2, 129.8, 130.8, 131.9, 134.6, 149.2, 150.2, 153.3, 153.7, 164.6; HRMS (ESI-TOF) Calcd for C $_{23}$ H $_{18}$ N $_2$ O $_4$ ([M + H] $^+$) 387.1300, found 387.1306. Anal. Calcd for C $_{23}$ H $_{18}$ N $_2$ O $_4$: C 71.49; H 4.70; N 7.25%. Found: C 71.46; H 4.66; N 7.29%.

2-Amino-4-(2-hydroxynaphthalen-1-yl)-4H-chromene-3-carbonitrile (4m). Yield: (0.292g, 93%); White crystalline solid; mp 212–214 °C; IR (KBr) 3360, 3228, 2987, 2214, 1627, 1599, 1479, 1393, 1191, 1169, 1037, 759 cm $^{-1}$; δ_H (300 MHz; DMSO- d_6 ; Me $_4$ Si) δ 5.10 (s, 1H), 6.06 (s, 2H), 6.31 (s, 1H), 6.82 (s, 2H), 7.05 (s, 2H), 7.26–7.64 (m, 4H), 10.80 (s, 1H); δ_C (75 MHz, DMSO- d_6 ; Me $_4$ Si) δ 30.2, 110.9, 118, 7, 119.0, 124.2, 124.4, 125.6, 125.8, 125.9, 126.1, 126.5, 126.8, 127.9, 128.3, 134.6, 138.5, 141.2, 143.6, 150.4; HRMS (ESI-TOF) Calcd for C $_{20}$ H $_{14}$ N $_2$ O $_2$ ([M + H] $^+$) 315.1089, found 315.1092. Anal. Calcd for C $_{20}$ H $_{14}$ N $_2$ O $_2$: C 76.42; H 4.49; N 8.91%. Found: C 76.37; H 4.47; N 8.88%.

9-(1H-Indol-3-yl)-3,3-dimethyl-2,3,4,9-tetrahydro-1H-xanthen-1-one (4n). Yield: (0.312g, 91%); Pale yellow crystalline solid; mp 117–119 °C; IR (KBr) 3444, 3330, 3087, 2954, 2910, 1705, 1633, 1587, 1484, 1410, 1365, 1199, 1148, 1087, 755 cm $^{-1}$; δ_H (300 MHz;

DMSO-*d*₆; Me₄Si) δ 0.82 (s, 3H), 0.95 (s, 3H), 1.93–2.25 (m, 2H), 2.38–2.46 (m, 2H), 5.06 (s, 1H), 6.25 (s, 1H), 6.49–7.36 (m, 8H), 10.48 (s, 1H); δ _C (75 MHz, DMSO-*d*₆; Me₄Si) δ 26.5, 26.9, 27.7, 28.7, 28.8, 31.5, 50.4, 111.0, 112.2, 114.9, 115.9, 118.2, 119.5, 120.6, 122.5, 123.4, 124.3, 125.2, 125.6, 126.4, 126.8, 126.9, 136.3, 136.5, 149.0, 154.1, 163.7, 195.8; HRMS (ESI-TOF) Calcd for C₂₃H₂₁N₂O₂ ([M + H]⁺) 344.1606, found 344.1602. Anal. Calcd for C₂₃H₂₁N₂O₂: C 80.44; H 6.16; N 4.08%. Found: C 80.49; H 6.15; N 4.04%.

5-(1H-Indol-3-yl)-1,3-dimethyl-1H-chromeno[2,3-d]pyrimidine-2,4(3H,5H)-dione (4o). Yield: (0.326g, 92%); White crystalline solid; mp 178–180 °C; IR (KBr) 3400, 3346, 3081, 2881, 1712, 1634, 1549, 1498, 1423, 1386, 1146, 1091, 756 cm⁻¹; δ _H (300 MHz; DMSO-*d*₆; Me₄Si) δ 3.00–3.11 (m, 3H), 3.30 (m, 3H), 5.24 (s, 1H), 6.45–6.53 (m, 2H), 6.55–6.71 (m, 2H), 6.73–7.34 (m, 4H), 10.72 (s, 1H); δ _C (75 MHz, DMSO-*d*₆; Me₄Si) δ 28.2, 29.4, 30.2, 111.8, 118.4, 118.5, 118.9, 119.4, 121.1, 123.9, 126.9, 127.3, 129.7, 137.0, 154.8, 163.4; HRMS (ESI-TOF) Calcd for C₂₁H₁₇N₃O₃ ([M + H]⁺) 360.1303, found 360.1299. Anal. Calcd for C₂₁H₁₇N₃O₃: C 70.18; H 4.77; N 11.69%. Found: C 70.15; H 4.79; N 11.64%.

2-Amino-4-(1H-indol-3-yl)-4H-chromene-3-carbonitrile (4p). Yield: (0.259g, 90%); White crystalline solid; mp 154–156 °C; IR (KBr); 3456, 3356, 2198, 1656, 1599, 1580, 1528 and 1409, 753 cm⁻¹; δ _H (300 MHz; DMSO-*d*₆; Me₄Si) δ 5.78 (s, 1H), 6.69–7.22 (m, 3H), 7.33–7.36 (m, 2H), 7.42–7.54 (m, 2H), 7.91–8.24 (m, 3H); δ _C (75 MHz, DMSO-*d*₆; Me₄Si) δ 28.6, 49.6, 104.5, 115.6, 115.9, 116.7, 117.3, 124.5, 128.7, 129.3, 133.8, 146.5, 152.4, 153.7; HRMS (ESI-TOF) Calcd for C₁₈H₁₃N₃O ([M + H]⁺) 288.1092, found 288.1091. Anal. Calcd for C₁₈H₁₃N₃O: C 75.25; H 4.56; N 14.63%. Found: C 75.21; H 4.52; N 14.59%.

4-(3,3-Dimethyl-1-oxo-2,3,4,9-tetrahydro-1H-xanthen-9-yl)-5-methyl-2-phenyl-1H-pyrazol-3(2H)-one (4q). Yield: (0.352g, 88%); Pale yellow crystalline solid; mp 242–244 °C; IR (KBr) 3080, 3061, 2988, 1659, 1598, 1490, 1387, 1198, 1039, 758 cm⁻¹; δ _H (300 MHz; DMSO-*d*₆; Me₄Si) δ 0.87 (s, 3H), 1.01 (s, 3H), 2.06–2.34 (m, 4H), 2.46 (s, 3H), 5.03 (s, 1H), 6.72–6.93 (m, 4H), 7.07–7.26 (m, 2H), 7.61–8.02 (m, 3H), 10.83 (s, 1H); δ _C (75 MHz, DMSO-*d*₆; Me₄Si) δ 26.4, 27.1, 32.5, 33.0, 53.0, 106.4, 111.3, 114.3, 115.4, 117.5, 118.3, 120.8, 123.8, 125.6, 126.1, 128.5, 131.1, 135.3, 145.7, 146.9, 151.9, 162.6, 196.7; HRMS (ESI-TOF) Calcd for C₂₅H₂₄N₂O₃ ([M + H]⁺) 401.1801, found 401.1798. Anal. Calcd for C₂₅H₂₄N₂O₃: C 74.98; H 6.04; N 7.04%. Found: C 74.94; H 6.07; N 7.09%.

5-Methyl-4-(1-oxo-2,3,4,9-tetrahydro-1H-xanthen-9-yl)-2-phenyl-1H-pyrazol-3(2H)-one (4r). Yield: (0.357g, 90%); White crystalline solid; mp 253–255 °C; IR (KBr) 3036, 3010, 1676, 1502, 1465, 1388, 1337, 1254, 1179, 1012, 762 cm⁻¹; δ _H (300 MHz; DMSO-*d*₆; Me₄Si) δ 2.09–2.12 (m, 2H), 2.27 (s, 3H), 3.64–3.93(m, 4H), 5.20 (s, 1H), 7.00–7.38 (m, 2H), 7.61–7.76 (m, 2H); δ _C (75 MHz, DMSO-*d*₆; Me₄Si) δ 17.6, 25.7, 27.6, 29.5, 33.6, 39.2, 105.8, 106.4, 115.8, 119.7, 123.3, 124.4, 125.8, 127.0, 128.0, 131.6, 140.7, 144.4, 152.6, 165.6, 197.1; HRMS (ESI-TOF) Calcd for C₂₃H₂₀N₂O₃ ([M + H]⁺) 373.1507, found 373.1515. Anal. Calcd for C₂₃H₂₀N₂O₃: C 74.18; H 5.41; N 7.52%. Found: C 74.17; H 5.37; N 7.57%.

4-(3,3-Dimethyl-1-oxo-2,3,4,9-tetrahydro-1H-xanthen-9-yl)-5-methyl-3H-pyrazol-3-one (4s). Yield: (0.289g, 90%); White crystalline solid; mp 165–167 °C; IR (KBr) 3455, 2190, 1666, 1609, 1548, 1487, 1405, 1022, 757 cm⁻¹; δ _H (300 MHz; DMSO-*d*₆; Me₄Si) δ 0.90 (s, 3H), 1.02 (s, 3H), 2.01–2.19 (m, 2H), 2.32–2.47 (m, 2H), 2.49 (s, 3H), 5.63 (s, 1H), 7.02–7.14 (m, 2H), 7.32–7.48 (m, 2H); δ _C (75 MHz, DMSO-*d*₆; Me₄Si) δ 25.6, 26.4, 27.8, 30.6, 49.0, 114.4, 115.4, 122.6, 126.2, 127.3, 129.9, 132.2, 151.8, 168.8, 196.1; HRMS (ESI-TOF) Calcd for C₁₉H₁₈N₂O₃ ([M + H]⁺) 323.1351, found 323.1348. Anal. Calcd for C₁₉H₁₈N₂O₃: C 70.79; H 5.63; N 8.69%. Found: C 70.79; H 5.60; N 8.65%.

5-Methyl-4-(1-oxo-2,3,4,9-tetrahydro-1H-xanthen-9-yl)-3H-pyrazol-3-one (4t). Yield: (0.344g, 89%); White crystalline solid; mp 188–190 °C; IR (KBr) 3455, 2988, 2198, 1656, 1622, 1576, 1466, 1456, 1021, 757 cm⁻¹; δ _H (300 MHz; DMSO-*d*₆; Me₄Si) δ 2.57–2.58 (m, 2H), 2.69 (s, 3H), 3.21–3.26 (m, 2H), 3.66 (s, 2H), 5.02 (s, 1H), 7.91–7.93 (m, 1H), 8.04–8.06 (m, 1H), 8.12–8.43 (m, 2H); δ _C (75 MHz, DMSO-*d*₆; Me₄Si) δ 25.7, 26.9, 27.3, 41.0, 49.5, 108.8, 120.4,

125.2, 127.7, 129.4, 131.7, 133.3, 135.5, 138.7, 157.6, 196.6; HRMS (ESI-TOF) Calcd for C₁₇H₁₄N₂O₃ ([M + H]⁺) 295.1038, found 295.1044. Anal. Calcd for C₁₇H₁₄N₂O₃: C 69.38; H 4.79; N 9.52%. Found: C 69.32; H 4.76; N 9.57%.

6-Amino-5-(3,3-dimethyl-1-oxo-2,3,4,9-tetrahydro-1H-xanthen-9-yl)pyrimidine-2,4(1H,3H)-dione (4u). Yield: (0.303g, 86%); White crystalline solid; mp >300 °C; IR (KBr) 3366, 3204, 2999, 2913, 1713, 1645, 1596, 1497, 1384, 1368, 1298, 969, 754 cm⁻¹; δ _H (300 MHz; DMSO-*d*₆; Me₄Si) δ 0.90 (s, 3H), 0.96 (s, 3H), 1.99–2.15 (m, 2H), 2.34–2.41 (m, 2H), 4.56 (s, 1H), 6.18 (s, 2H), 6.79–6.99 (m, 4H), 9.75 (s, 1H), 9.86 (s, 1H); δ _C (75 MHz, DMSO-*d*₆; Me₄Si) δ 25.1, 27.1, 29.6, 33.6, 106.1, 116.6, 115.4, 118.6, 120.4, 123.1, 126.5, 127.7, 128.9, 131.1, 135.6, 139.6, 151.9, 163.6, 197.2; HRMS (ESI-TOF) Calcd for C₁₉H₁₉N₃O₄ ([M + H]⁺) 354.1409, found 354.1413. Anal. Calcd for C₁₉H₁₉N₃O₄: C 64.58; H 5.42; N 11.89%. Found: C 64.57; H 5.37 N 11.93%.

5-(6-Amino-2,4-dioxo-1,2,3,4-tetrahydropyrimidin-5-yl)-1,3-dimethyl-1H-chromeno[2,3-d]pyrimidine-2,4(3H,5H)-dione (4v). Yield: (0.313g, 85%); White crystalline solid; mp >300 °C IR (KBr) 3466, 3236, 2991, 2944, 1703, 1656, 1567, 1491, 1386, 1293, 1066, 759 cm⁻¹; δ _H (300 MHz; DMSO-*d*₆; Me₄Si) δ 3.22 (s, 3H), 3.45 (s, 3H), 5.51 (s, 1H), 6.97–7.18 (m, 4H), 7.36 (t, J = 7.5 Hz, 1H), 7.37–7.85 (m, 2H); δ _C (75 MHz, DMSO-*d*₆; Me₄Si) δ 20.4, 27.6, 28.6, 36.9, 114.9, 116.7, 118.4, 120.1, 123.8, 125.0, 127.6, 129.3, 130.0, 147.7, 153.7, 166.9, 197.9; HRMS (ESI-TOF) Calcd for C₁₇H₁₅N₅O₅ ([M + H]⁺) 370.1107, found 370.1104. Anal. Calcd for C₁₇H₁₅N₅O₅: C 55.28; H 4.09 N 18.96%. Found: C 55.28; H 4.09 N 18.96%.

■ ASSOCIATED CONTENT

Supporting Information

ORTEP drawings of compounds **4e**, ¹H and ¹³C NMR spectra of all compounds, and X-ray data for compounds **4e** in CIF format. These materials are available free of charge via the Internet at <http://pubs.acs.org>.

■ AUTHOR INFORMATION

Corresponding Author

*E-mail: ardchem@caluniv.ac.in, ardas66@rediffmail.com. Tel.: +913323501014, +919433120265. Fax: +913323519754.

Notes

The authors declare no competing financial interest.

■ ACKNOWLEDGMENTS

We gratefully acknowledge the financial support from U.G.C. and University of Calcutta. P.P.G. thanks U.G.C., New Delhi, India, for the grant of his Senior Research Fellowship. Crystallography was performed at the DST-FIST, India-funded Single Crystal Diffractometer Facility at the Department of Chemistry, University of Calcutta. We also gratefully acknowledge the TEQIP and Indian Association for the Cultivation of Science for instrument facilities, and thanks are also extended to Mr. Dibyendu Mondal for his various cooperation.

■ REFERENCES

- (1) (a) Anastas, P. T.; Warner, J. C. *Theory and Practice*. In *Green Chemistry*; Oxford University Press: Oxford, U.K., 1998. (b) Anastas, P. T.; Williamson, T. *Frontiers in Benign Chemical Synthesis and Process*. In *Green Chemistry*; Oxford University Press: Oxford, U.K., 1998.
- (2) (a) *Organic Reactions in Water: Principles, Strategies and Applications*; Lindstrom, U. M., Ed.; Blackwell Publishing: Oxford, U.K., 2007. (b) Weber, L. *Drug Discovery Today* **2002**, *7*, 143. (c) Domling, A. *Chem. Rev.* **2006**, *106*, 17.
- (3) (a) *Multicomponent Reactions*; Zhu, J., Bienayme, H., Eds.; Wiley-VCH Verlag GmbH & Co.: Weinheim, Germany, 2005. (b) Chanda, A.; Fokin, V. V. *Chem. Rev.* **2009**, *109*, 725.

- (4) (a) Reetz, M. T.; Lohmer, G. *Chem. Commun.* **1996**, 1921. (b) Reetz, M. T.; Westermann, E. *Angew. Chem., Int. Ed.* **2000**, *39*, 165. (c) Ramarao, C.; Ley, S. V.; Smith, S. C.; Shirley, I. M.; De Almeida, N. *Chem. Commun.* **2002**, 1132.
- (5) (a) Gladysz, J. A. *Pure Appl. Chem.* **2001**, *73*, 1319. (b) Gladysz, J. A. *Chem. Rev.* **2002**, *102*, 321. (c) Sheldon, R. A.; Arends, I.; van Rantwijk, F. *Green Chemistry and Catalysis*; John Wiley: Weinheim, Germany, 2006. (d) Ding, K.; Uozumi, Y. *Handbook of Asymmetric Heterogeneous Catalysis*; Wiley-VCH: Weinheim, Germany, 2008. (e) Bartok, M. *Chem. Rev.* **2010**, *110*, 1663.
- (6) (a) Ellis, G. P.; Lockhart, I. M. In *The Chemistry of Heterocyclic Compounds: Chromenes, Chromanones, and Chromones*; Ellis, G. P., Ed.; Wiley-VCH: Weinheim, Germany, 2007; Vol. 31, pp 1–1196. (b) Geen, G. R.; Evans, J. M.; Vong, A. K. In *Comprehensive Heterocyclic Chemistry II: Pyrans and Their Benzo Derivatives: Applications*; Katritzky, A. R., Rees, C. W., Scriven, E. F. V., Eds.; Pergamon Press: Oxford, U.K., 1996; Vol. 5, pp 469–500.
- (7) El-Nagger, A. M.; Abdel-El-Salam, A. M.; Latif, F. S. M.; Ahmed, M. S. A. *Pol. J. Chem.* **1981**, *55*, 793.
- (8) Ohemeng, K. A.; Schwender, C. F.; Fu, K. P.; Barrett, J. F. *Bioorg. Med. Chem. Lett.* **1993**, *3*, 225.
- (9) Middleton, E.; Kandaswami, C. The Impact of Plant Flavonoids on Mammalian Biology. Implication for Immunity, Inflammation and Cancer. In *The Flavonoids Advances in Research Since 1986*; Harborne, J. B., Ed.; Chapman Hall: London, U.K., 1994; p 619.
- (10) (a) Foye, W. O. *Principi Di Chemico Farmaceutica*; Piccin: Padova, Italy, 1991; p 416. (b) Andreani, L. L.; Lapi, E. *Bull. Chim. Farm.* **1960**, *99*, 583. (c) Bonsignore, L.; Loy, G.; Secci, D.; Calignano, A. *Eur. J. Med. Chem.* **1993**, *28*, 517.
- (11) Park, C.; Lim, C.-Y.; Kim, J.-H.; Jang, J. -I.; Park, H.-M. *Can. Vet. J.* **2011**, *52*, 165.
- (12) Lo, V. M.; Ching, C. K.; Chan, A. Y.; Mak, T. W. *Clin. Toxicol.* **2008**, *46*, 703.
- (13) Fry, J. C.; Yurttas, N.; Biermann, K. L.; Lindley, M. G.; Goulson, M. J. *J. Food. Sci.* **2012**, *77*, 362.
- (14) Gobel, H.; Heinze, A.; Niederberger, U.; Witt, T.; Zumbroich, V. *Cephalalgia* **2004**, *24*, 888.
- (15) Burdan, F. *Hum. Exp. Toxicol.* **2004**, *23*, 235.
- (16) Chen, W.; Cai, Y.; Fu, X.; Liu, X.; Lin, L.; Feng, X. *Org. Lett.* **2011**, *13*, 4910.
- (17) Li, M.; Gu, Y. *Adv. Synth. Catal.* **2012**, *354*, 2484.
- (18) Li, M.; Zhang, B.; Gu, Y. *Green Chem.* **2012**, *14*, 2421.
- (19) (a) Das, V. K.; Devi, R. R.; Raul, P. K.; Thakur, A. J. *Green Chem.* **2012**, *14*, 847. (b) Das, V. K.; Borah, M.; Thakur, A. J. *J. Org. Chem.* **2013**, *78*, 3361.
- (20) (a) Ghosh, P. P.; Pal, G.; Paul, S.; Das, A. R. *Green. Chem.* **2012**, *14*, 2691. (b) Ghosh, P. P.; Mukherjee, P.; Das, A. R. *RSC Adv.* **2013**, DOI: 10.1039/C3RA40706C. (c) Bhattacharyya, P.; Paul, S.; Das, A. R. *RSC Adv.* **2013**, *3*, 2203. (d) Ghosh, P. P.; Paul, S.; Das, A. R. *Tetrahedron Lett.* **2013**, *54*, 138. (e) Paul, S.; Bhattacharyya, P.; Das, A. R. *Tetrahedron Lett.* **2011**, *52*, 4636. (f) Ghosh, P. P.; Das, A. R. *Tetrahedron Lett.* **2012**, *53*, 3140. (g) Bhattacharyya, P.; Pradhan, K.; Paul, S.; Das, A. R. *Tetrahedron Lett.* **2012**, *53*, 4687.
- (21) (a) Rema Devi, B. S.; Raveendran, R.; Vaidyan, A. V. *Pramana* **2007**, *68*, 679. (b) John, R.; Florence, S. S. *Chalcogenide Lett.* **2010**, *7*, 269. (c) Zhang, H.; Gilbert, B.; Huang, F.; Banfield, J. F. *Nature* **2003**, *424*, 1025.
- (22) Crystallographic data (excluding structure factors) for **4e** have been deposited with the Cambridge Crystallographic Data Center as supplementary publication number CCDC 926789 (see also ESI).